Journal of Power Sources 189 (2009) 81–88

Contents lists available at ScienceDirect

Journal of Power Sources

journal homepage: www.elsevier.com/locate/jpowsour

Electrochemical activity of Li_2FeTiO_4 and Li_2MnTiO_4 as potential active materials for Li ion batteries: A comparison with Li_2NiTiO_4

Mirjana Küzma[a], Robert Dominko[a], Anton Meden[b], Darko Makovec[c], Marjan Bele[a], Janko Jamnik[a], Miran Gaberšček[a,b,*]

[a] National Institute of Chemistry, Ljubljana, Slovenia
[b] Faculty of Chemistry and Chemical Technology, University of Ljubljana, Slovenia
[c] Jožef Stefan Institute, Ljubljana, Slovenia

ARTICLE INFO

Article history:
Received 24 July 2008
Received in revised form 4 November 2008
Accepted 5 November 2008
Available online 13 November 2008

Keywords:
Li ion batteries
Cathode
Titanates
Li_2FeTiO_4
Li_2NiTiO_4
Carbon coating

ABSTRACT

We demonstrate, for the first time, a considerable electrochemical activity of two members of lithium transition element titanates: Li_2FeTiO_4 and Li_2MnTiO_4. Both materials consist of 10–20 nm particles embedded in a conductive carbon coating. We show that not the coating but the small particle size is decisive for materials' activity. Li_2FeTiO_4 shows a stable reversible capacity of up to 123 mA hg^{-1} at C/20 and 60 °C which is 83% of the theoretical value for exchange of 1 electron (148 mA hg^{-1}). Li_2MnTiO_4 could only be prepared in a nanosized form that contained about 30% of impurities. The capacity of the whole material (including impurities) is comparable to that of Li_2FeTiO_4 but the cycling stability is much poorer. In contrast to the Fe and Mn analogues, the third member of the titanate family, Li_2NiTiO_4, shows a good electrochemistry even when the particle size is much larger (about 100 nm). During initial cycles at C/10 and 60 °C, exchange of more than 1 electron per compound formula has been observed. The cycling stability at high temperatures, however, is poor.

1. Introduction

Introduction of novel synthesis approaches that allow for controlled materials nanostructurization have helped launch a range of interesting new insertion materials for potential use in lithium batteries. In particular, nanostructurization has led to efficient utilization of olivine phosphates [1–3] and even exploitation of silicates [4,5] that are traditionally known as highly insulating materials. A precondition for utilization of such low-conductivity materials (<10^{-10} S cm^{-1} at RT) is that their typical dimension is not larger than several tens of nanometers. Thereby, all the materials surface area must be easily accessible for electrons and ions from the respective reservoirs. In other words, no significant agglomeration of phases should occur and, additionally, percolated conductive paths for both ions and electrons have to be provided within the whole composite electrode material. An effective way for preparation of such nanoarchitectures is the use of carbon precursors, such as citric acid [6] which during thermal treatment transform into conductive carbon coatings. On one hand, the presence of carbon suppresses both the particle growth and agglomeration during the synthesis [7]; on the other hand, the carbon can serve as a percolated electron conductor which, at the same time, is also permeable for lithium ions [6].

In this work, we use the carbon precursor approach for preparation of novel active materials from the family of transition metal (M) titanates, Li_2MTiO_4. The titanates could be quite interesting insertion materials because the presence of Ti^{4+}, which forms strong bonds with oxygen, could favour stabilization of the M^{3+}/M^{2+} transition [8]. Several members from the titanate family have already been successfully synthesized (M = Mg, Mn, Fe, Co, Ni) and characterized with respect to their structure, microstructure, conductivity, chemical, dielectric and magnetic properties [8–11]. In all cases, a disordered rock-salt-type structure was unambiguously determined. The electric conductivity has only been determined for Li_2MgTiO_4—at temperatures above 400 °C [10]; extrapolating the data to room temperature, one gets a very low conductivity of ca. 10^{-10} S cm^{-1}. Neither the electronic nor the ionic conductivities for the other titanates have been reported. If either conductivity type is low (on the order of 10^{-10} S cm^{-1} or lower), then the titanates have to be prepared in a form of very small particles (on the order of 100 nm or smaller) to show a reasonable electrochemical activity [12]. If solely the electronic conductivity is low, preparation of conductive carbon coatings should be helpful as well [12].

* Corresponding author at: National Institute of Chemistry, Ljubljana, Slovenia. Tel.: +386 1 4760322; fax: +386 1 476422.
E-mail address: miran.gaberscek@ki.si (M. Gaberšček).

0378-7753/$ – see front matter © 2008 Elsevier B.V. All rights reserved.
doi:10.1016/j.jpowsour.2008.11.015

Until now, only the Li_2NiTiO_4 analogue has been electrochemically tested [8]. The majority of particles had a typical dimension between 50 and 100 nm. The first-cycle reversible capacity was significant (almost 100 mA hg^{-1} at C/2) but the cycleability was not reported. Here we show, for the first time, that by preparing even smaller particles (10–20 nm), it is possible to electrochemically exploit also other members of titanates, in particular Li_2FeTiO_4 and Li_2MnTiO_4. We also discuss in some detail the main differences between all the three members of the titanate family.

2. Experimental

The synthesis of all materials was based on a patented citrate-precursor method [13]. 0.002–0.02 mol of titanium(IV) oxide, anatase (Aldrich, 637254) was dispersed in 9.7–97 mL miliQ using an ultrasound bath. After addition of 0.004–0.04 mol of lithium hydroxide (99%, Aldrich, 442410) the mixture was maintained in the ultrasound bath for another hour. (In the case of manganese analogue, lithium acetate dihydrate, bioUltra, 99%, Fluka, 62393 was used.) Separately, 0.002–0.02 mol of iron(III) citrate hydrate (98%, Aldrich F6129) was dissolved in 9.5–95 mL miliQ water at 60 °C. (In the case of manganese analogue, manganese(II) acetate tetrahydrate, purum p.a., Aldrich, 63537 was used. We also added 0.02 mol of citric acid, 99%, Aldrich, C83155 and 0.06 mol of ethylene glycol, anhydrous, 99.8%, Aldrich, 324558. In the case of nickel analogue, Nickel(II) acetate tetrahydrate, purum p.a., Aldrich, 72225 was used.)

After cooling to room temperature, both solutions were mixed and then partly dried at 60 °C to obtain a viscous liquid. Then, the material was additionally kept in a drier overnight at 60 °C under vacuum to obtain a dry powder. After thorough grinding with a mortar and pestle, the obtained xerogels were heat-treated in a gas-tight quartz tube with a constant flow of appropriate gas. The obtained xerogels were heat-treated in different atmospheres: the Fe analogue was heated in a mixture of CO/CO_2 (1:1) gases, the Mn analogue was heat-treated in a constant flow of argon gas and Ni analogue in the air. Only the latter sample did not contain in situ carbon. The initial heating rate was 5 °C min^{-1} until reaching 700 °C.

For preparation of pure Li_2FeTiO_4, the procedure was modified in two ways: (1) instead of lithium hydroxide, lithium nitrate (99.9%, Merck, 1056530100) was used and (2) iron(III) citrate hydrate was replaced by iron(III) nitrate nonahydrate (purum p.a., 97%, Fluka 44952).

In one series, the pure Li_2FeTiO_4 was coated by a thin carbon coating using the following procedure [7]. 1 g of the as-obtained pure Li_2FeTiO_4 was mixed with 150 mg of citric acid (99%, Aldrich, C83155) and grinded with a mortar and pestle for 30 min inside a glove box. The obtained mixture was heat-treated at a constant flow of CO/CO_2 gas (1:1). The initial heating rate was 2.5 °C min^{-1} until reaching 700 °C.

Surfaces of samples were observed and analyzed with a field-emission scanning electron microscope (Supra 35 VP, Carl Zeiss) at an accelerating voltage of 1 kV. In the case of Li_2FeTiO_4 and Li_2MnTiO_4, the X-ray measurements were performed in a capillary (0.3 mm diameter) to prevent the oxidation of the materials. The measurements were carried out on a PANalytical X'pert PRO MPD powder diffractometer in a transmission mode using parallel beam optics (hybrid monochromator) with Cu Kα_1 radiation. The data were collected in the range $30° \leq 2\theta \leq 135°$ in steps of 0.033° and the integration time of 72 s per step. Because Li_2NiTiO_4 is much more stable in air conditions, the X-ray powder diffraction pattern of this material was collected under usual conditions (capillary was not needed) on a Siemens D-5000 diffractometer in reflection (Bragg–Brentano) mode using Cu Kα_1 radiation, monochromatized by a secondary graphite monochromator. The data were collected in the range between 15 and 70° in steps of 0.04° and the integration time of 1 s per step.

For TEM investigations the materials were deposited on a copper-grid-supported perforated transparent carbon foil. A field-emission electron-source transmission electron microscope TEM (JEOL 2010 F), equipped with an energy dispersive X-ray spectroscopy (EDS) system (LINK, ISIS EDS 300) was used.

For electrochemical measurements, the samples were grinded with 10 wt.% of added acetylene black and 10% of binder and then pressed onto a circular Al foil with a diameter of 16 mm (2 cm^2). The active material mass was always between 5 and 6 mg. The electrochemical characteristics were measured in vacuum-sealed triplex foil (coffee bag foil) cells. The electrolyte used was a 0.8 M solution of LiBOB (Chemetall) in EC:DEC (1:1 ratio by volume) purchased from Aldrich. Solvents and salt were used as received. The working electrode and the counter electrode consisting of metallic lithium were separated with a glass wool separator. The electrochemical measurements were performed using a VMP3 potentiostat/galvanostat at a constant temperature of 60 °C and at room temperature with a current density corresponding to C/10 or C/2. The capacities are always defined as discharge capacities and calculated per mass of pure active material (subtracting the content of native carbon and other additives) unless stated otherwise.

Conductivity measurements were carried out on isostatically pressed samples at 750 MPa for 30 s. On the surface of pellets gold contacts were sputtered. The samples were inserted into a gas-tight quartz cell allowing for precise control of atmosphere and temperature up to 1000 °C. Pure nitrogen atmosphere was used in this particular case. The impedance spectra at different temperatures were recorded with a Hewlet Packard 4284 A instrument, in a frequency range of 1 MHz to 20 Hz.

3. Results and discussion

3.1. General features of prepared titanates

As mentioned in Introduction, our main goal was to prepare and electrochemically test Li_2FeTiO_4 and Li_2MnTiO_4. However, we soon realized that these two analogues showed extremely poor reversible capacity (10–20 mA hg^{-1}) if prepared in a similar way as the earlier reported nickel analogue [8]. To improve the capacity of Fe and Mn compounds, we decided to follow our strategy used earlier on several other cathode materials [6,7,14] which involves either preparation of carbon coatings around the active particles and/or significant reduction of the particle dimension. Indeed, this strategy has appeared successful also in titanates, as shown in continuation. To demonstrate the main concept, we here focus on 5 crucial samples (Table 1) with different compositions and different morphologies.

The first material (Fig. 1a) is Li_2NiTiO_4 with characteristics very similar to those reported by Prabaharan et al. [8]. This material is denoted as LNT100 whereby the number "100" indicates the estimated mean particle size in nanometres (see Table 1). The main purpose of LNT100 is to serve as a reference material, to which the other materials are compared. The next material (Fig. 1b) is LFT150—a Fe analogue with a morphology roughly comparable to the Ni analogue (estimated mean particle size is about 150 nm). The third material (Fig. 1c) is the same Fe analogue but coated afterwards with a carbon coating (CC) using a well-established procedure [8]; it is thus designated as LFT150_CC. The fourth material (Fig. 1d) is again a carbon-coated Li_2FeTiO_4 but prepared according to the full citrate-precursor method as described in Section 2. The essential feature of this material, designated as LFT20_CC, is that the mean particle size is much smaller, about 20 nm (obtained from Scherrer's formula; the actual size seen by optical methods varies

Table 1
Selected morphological and electrochemical data for the 5 titanate samples studied in this work. "LNT", "LFT" and "LMT" denote Li_2NiTiO_4, Li_2FeTiO_4 and Li_2MnTiO_4, respectively. "CC" denotes the presence of carbon coating. The capacities in column 6 are defined as discharge capacities whereby only the mass of active compound is considered (except in the last case). In all cases, the data are given for the 2nd cycle.

Sample	Estimated particle size range [nm]	Estimated mean particle size [nm]	Presence of native carbon	Theoretical capacity (1 electron reaction) [mA h g^{-1}]	Highest capacity observed in this work [mA h g^{-1}]
LNT100	50–150	100	No	145.3	179
LFT150	50–200 (individual particles up to 400 nm)	150	No	147.6	12
LFT150_CC	50–200 (individual particles up to 400 nm)	150	No (but coated afterwards)	147.6	14
LFT20_CC	10–25	20	Yes	147.6	123
LMT20_CC	10–25	20	Yes	148.3	132 (impurities included) 188 (impurities excluded)

from ca. 10 to 25 nm). The growth of size is presumably suppressed by the constant presence of carbon precursor during heating in an inert or slightly reductive atmosphere [8]. The fifth material (Fig. 1e) is a manganese analogue of the fourth material, that is, LMT20_CC—again prepared by the full citrate-precursor method.

Like in previous studies, the existence of carbon coatings on the materials was checked using TEM, an example is shown in Fig. 1f. In all cases the estimated coating thickness was about 1–4 nm. Additionally, the total amount of native carbon was determined using thermogravimetry. The values found were 15 and 11 wt.% for the LFT20_CC and LMT20_CC material, respectively. In the case of LFT150_CC with much bigger average particle size, the content of thin carbon coating was expectedly smaller—about 3 wt.%.

The structure of all three analogues, regardless of the synthesis method, was found to be the cubic rock-salt structure (space group *Fm*-3*m*)—the same as found in all previous reports dealing with the Li_2MTiO_4 (M = Mg, Mn, Fe, Co, Ni) family of compounds [8–11]. Fig. 2 shows examples of diffraction patterns for LNT100,

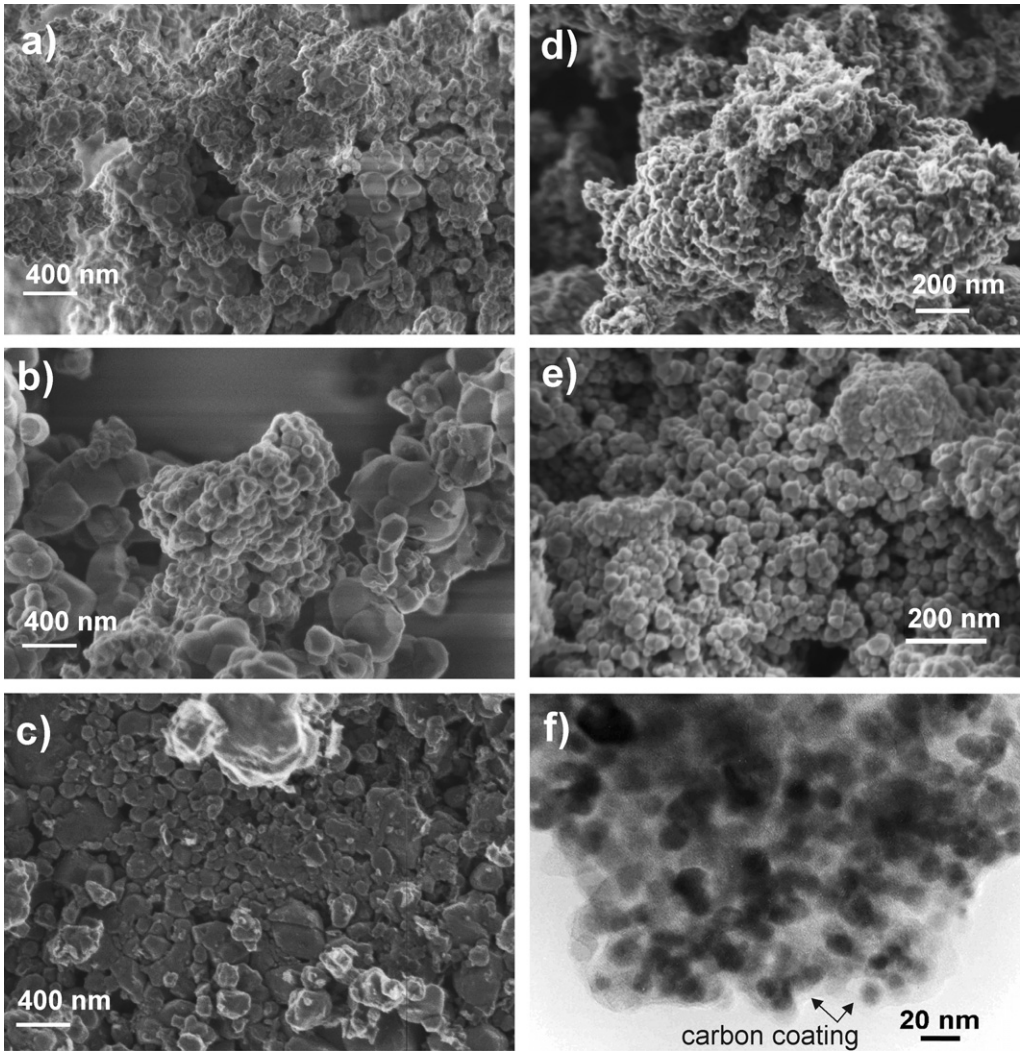

Fig. 1. Typical SEM photographs of as prepared samples: (a) LNT100, (b) LFT150, (c) LFT150_CC, (d) LFT20_CC and (e) LMT20_CC. (f) TEM photograph of LFT20_CC showing the presence of carbon coating. LNT, LFT and LMT designate Li_2NiTiO_4, Li_2FeTiO_4 and Li_2MnTiO_4, respectively. The numbers designate the average particle size and "CC" stands for presence of carbon coating.

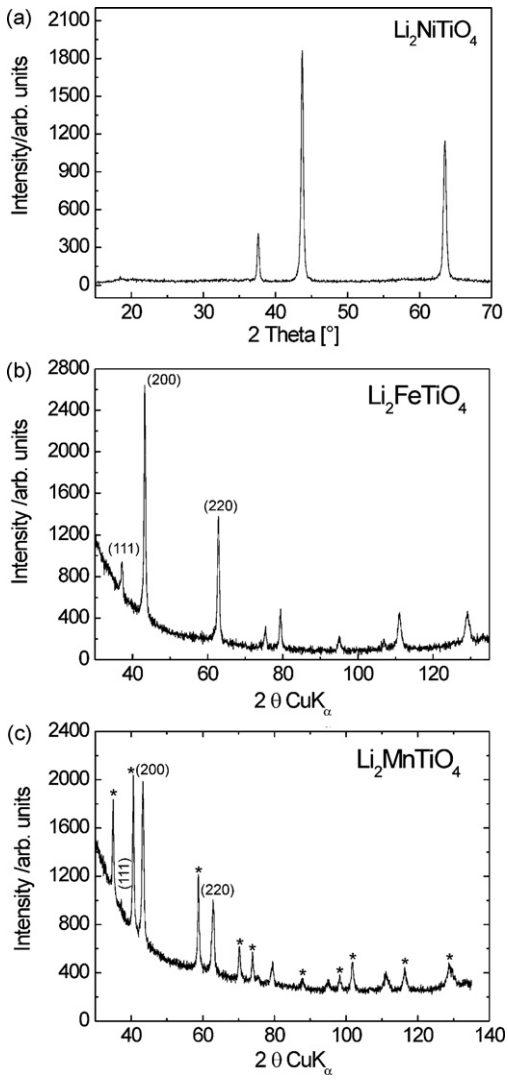

Fig. 2. XRD patterns of as-prepared (a) Li_2NiTiO_4 (LNT100), (b) Li_2FeTiO_4 (LFT20_CC) and (c) Li_2MnTiO_4 (LFT20_CC) materials. The asterisks denote the peaks due to MnO impurity in the Li_2MnTiO_4 material. The new active materials (nanosized Fe and Mn analogue) were recorded in capillary (to prevent sample oxidation) while the well-known Ni analogue with much bigger particles was measured using a standard Al carrier (hence the different scales and the different conditions).

LFT20_CC and LMT20_CC. While the former two samples are quite pure, the manganese analogue shows a considerable presence of the MnO impurity (marked with asterisks). A chemical analysis indicated that in this sample the total amount of impurities was about 30 wt.%.

The general electrochemical activity of Li_2NiTiO_4 was demonstrated and discussed in some detail by Prabaharan et al. [8]. Here we extend those findings to the Fe and Mn analogue. The most reproducible cyclic voltammograms were obtained with samples LFT20_CC and LMT20_CC. The general activity of these two samples was first probed in a wide potential window (Fig. 3a and b, scan rate = 0.1 mV s^{-1}). In the case of LFT20_CC (Fig. 3a), an oxidation and a reduction peak are observed at potentials between 2.5 and 2.9 V and between 2.1 and 2.5 V, respectively. For LMT20_CC (Fig. 3b), the cyclic voltammogram is much more complex. Reliable assignation of the various peaks is a matter of extensive future research but the transition Mn^{2+}/Mn^{3+} is certainly expected in this region. At higher voltages, the transition Mn^{3+}/Mn^{4+} is also possible—at least this would explain certain galvanostatic results (see Fig. 7). In both materials the processes below ca. 1.95 V were attributed to irreversible surface reactions so this region was cut off in further experiments. The upper potential limit was kept as high as possible to allow for the potential exchange of more than 1 electron (transition from M^{3+} to M^{4+}). Windows that were still found acceptable in terms of stability were as follows: between 1.95 and 3.9 V for LFT20_CC (Fig. 3c) and 1.95 and 4.8 V for LMT20_CC (Fig. 3d). These windows were then used in all further studies, except when stated otherwise. In the case of the reference LNT100 material, which was found less sensitive to the choice of potential window, we decided to use the same window as in the case of the manganese analogue (for easier comparison).

3.2. Influence of materials morphology on the electrochemistry of titanates

Fig. 4a compares the second charge–discharge curves for LNT100 and LFT150. Both materials have the same structure, are of similar purity (about 2–4% of impurities), only the particle size is somewhat different. The performance at the same external conditions (C/10, 60 °C, 2nd cycle), however, is very different. While the reversible capacity of LNT100 is about 153 mA hg^{-1} (corresponding to exchange of 1.05 Li per 1 mol of Li_2NiTiO_4), the reversible capacity of LFT150 is merely 12 mA hg^{-1} (about 0.08 Li per 1 mol of Li_2FeTiO_4). This extreme difference in behaviour cannot be explained neither by the somewhat bigger particles in LFT150 nor by the somewhat narrower potential window for this material. In order to improve the very poor behaviour of Li_2FeTiO_4, we first coated it by a 1–2 nm thick carbon film thus obtaining the material LFT150_CC. As seen from Fig. 4b, however, the reversibly capacity of LFT150_CC is only slightly higher than that of LFT150 (14 mA hg^{-1} vs. 12 mA hg^{-1}, respectively). In the next attempt, we used the full citrate-precursor sol–gel method to obtain sample LFT20_CC, that is, carbon-coated Li_2FeTiO_4 with particle size of merely 10–25 nm. Now the reversibly capacity increased to 83 mA hg^{-1} (about 0.56 Li per 1 mol of Li_2FeTiO_4). An obvious conclusion from Fig. 4b would be that reduction of the particle size is much more important for improvement of the capacity of Li_2FeTiO_4 than the conductive carbon coating. We have shown in our previous investigation on a $LiFePO_4$ material that such a behaviour is expected for active materials in which the electronic conductivity is higher than the ionic [12]. While for determination of the ionic conductivity one in principle needs a relatively big single crystal [15] (not available in this study), the measurement of electronic conductivity can be performed on a compact pellet of pure active material. We measured impedance spectra of isostatically pressed LFT150 and LNT100 pellets as functions of temperature. Extraction of conductivity data from the impedance data was carried out in the same way as previously described for other materials [7,16]. The obtained Arrhenius plots for both materials are shown in Fig. 5. At room temperature, the conductivity of LNT is about 10^{-8} S cm^{-1}, that is, about a decade higher than in the case of $LiFePO_4$ [7]. Quite surprisingly, the electronic conductivity of LFT150 is much higher, at RT the value is about 10^{-1} S cm^{-1}. These data lead clearly to the following conclusion: if the electrochemical behaviour of various titanates were determined by the electronic conductivity, LFT150 should perform much better than LNT100—just the opposite as shown in Fig. 4a. In other words, it is the ionic conductivity that determines the chemical diffusion rate inside these materials. That is why the conductive coating is not helpful. For the same reason, the particles not only have to be small but also have to be well separated from each other (to allow for full ionic contacting).

Unfortunately, we were not able to determine the electronic conductivity for the manganese analogue because, as mentioned above, this sample contained about 30% of impurities. We speculate, however, based on the relatively good electronic conductivity of LNT (Fig. 5) and on the electrochemical similarity between LNT and LMT

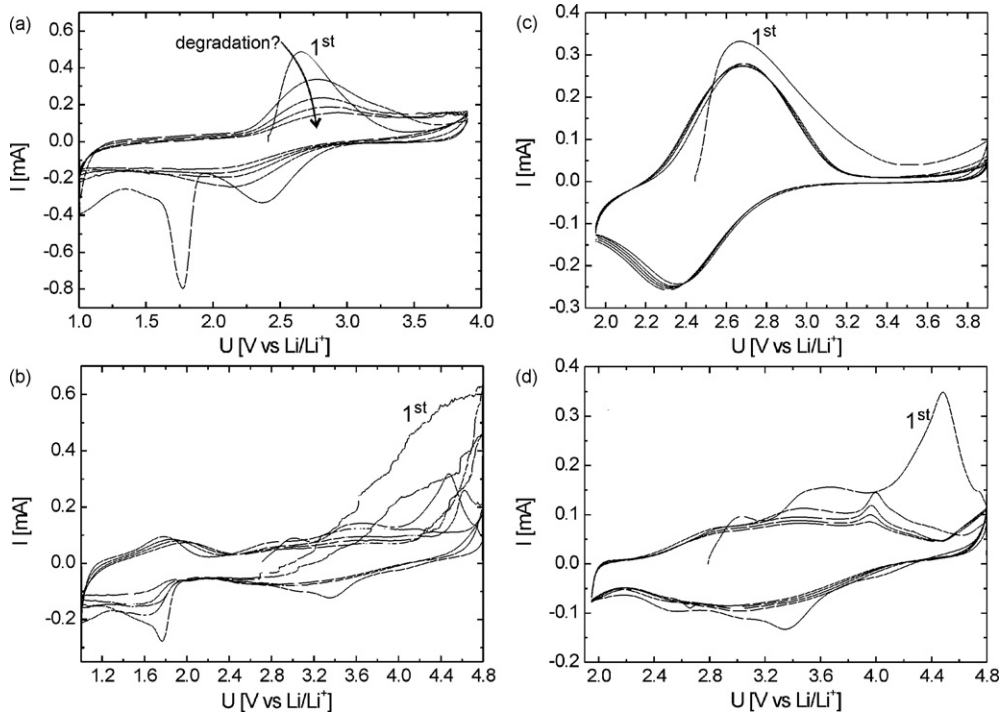

Fig. 3. Cyclic voltammograms of the prepared Li_2FeTiO_4 (a, c) and Li_2MnTiO_4 (b, d) samples. The scan rate was 0.1 mV/s. Each figure shows 5 consecutive cyclic voltammograms starting with the one labelled "1st".

(see below) that these two analogues also exhibit a higher electronic conductivity than the ionic. Similarly, the fact that the Fe and Mn analogues require much smaller particle size for a reasonable electrochemical activity than the Ni analogue could be explained by a lower ionic conductivity of the former two compounds. Further experiments are needed to confirm these hypotheses.

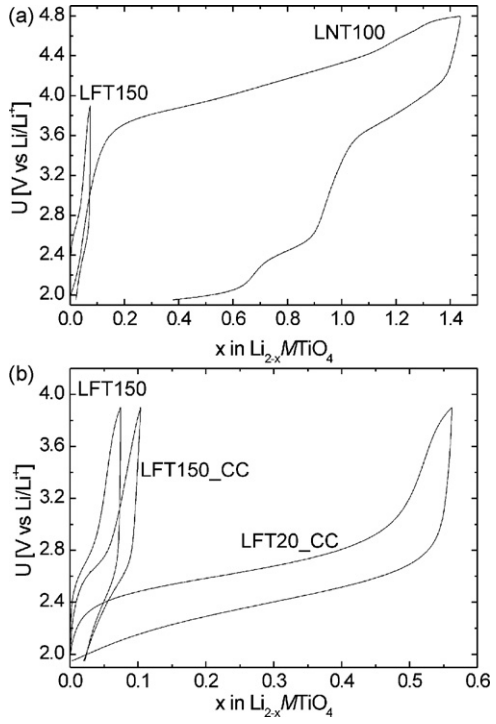

Fig. 4. (a) The second charge–discharge curves for LNT100 and LFT150. (b) The second charge–discharge curves for LFT150, LFT150_CC, and LFT20_CC. In all cases the rate was C/10 and the temperature 60 °C.

3.3. Influence of temperature on the electrochemical behaviour

Due to the very low performance of many initial titanate samples we mainly carried out the electrochemical experiments at 60 °C. After obtaining better samples, however, we also checked the activity at RT for all samples. Some unusual effects were observed, as seen on the examples shown in Fig. 6, which compares the results for all three compounds at C/2. Only the Fe analogue (sample LFT20_CC; Fig. 6b and e) shows the expected temperature effect: the performance at 60 °C is significantly better during all cycles. In the case of the other two samples, one common trend is a rapid degradation of capacity during cycling at 60 °C. So, even if in initial cycles the performance at 60 °C is expectedly better, it rapidly becomes comparable to or even lower than the performance at RT (see Fig. 6d and f). In further tests (not shown) we found that this degradation was especially pronounced at higher rates (C/2 and

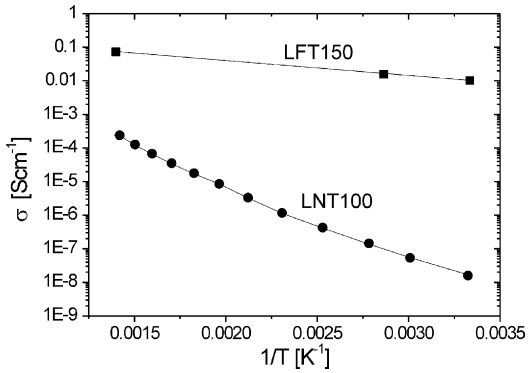

Fig. 5. Arrhenius plots for isostatically pressed LNT100 and LFT150 pellets. The pellet thickness was 1 mm. The very high conductivity of LFT150 is attributed to oxygen understoichiometry that probably occurs in nitrogen atmosphere (that is, at low oxygen partial pressure). Such an atmosphere, however, is also typical for coffee bag cells in which our experiments are carried out, so the results may be considered realistic.

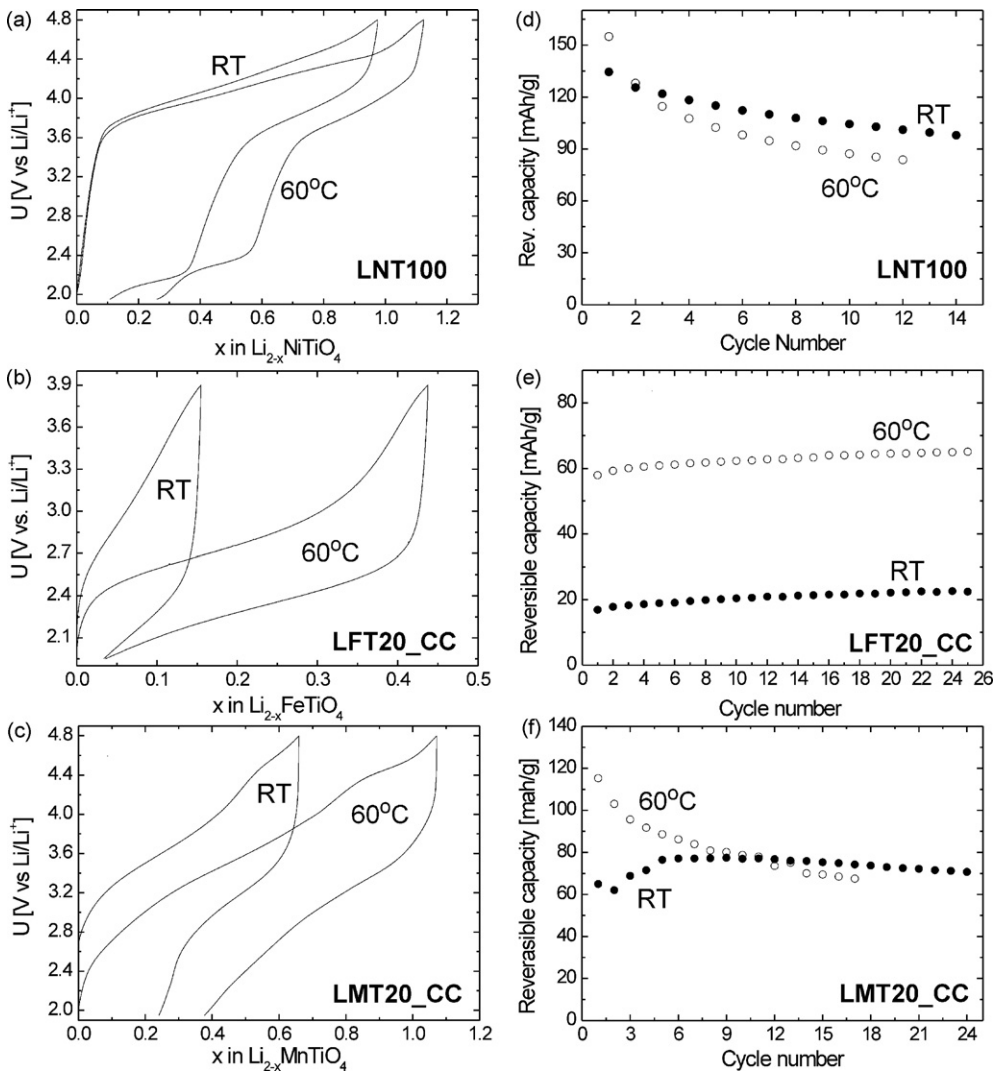

Fig. 6. Comparison of the titanate performance at 60 °C and at RT. The rate was always C/2 (in the Mn analogue the impurities were considered part of active material). The galvanostatic curves on the left correspond to the second cycles. The meaning of labels is explained in caption of Fig. 1 and in Table 1.

1 C) while at lower rates (C/10 and C/20) the degradation was less severe. At present, it is unclear why the Fe analogue is much more stable at higher temperatures than the other two analogues.

3.4. Which is the potential of titanates for use of cathodes for Li batteries?

Fig. 7 shows the best results obtained so far for all three analogues. The specific materials tested were LNT100, LFT20_CC and LMT20_CC, the rate was C/10 and the temperature 60 °C. In the case of the manganese analogue two curves are shown: the solid circles correspond to the calculation where impurities are considered as part of the active material and the open circles show the calculation in which the impurities (30%) are considered inactive and are thus subtracted. Note that in this case, as well as in the case of LNT100 (squares), the initial two or three points exceed the reversible capacity corresponding to the exchange of 1 mol Li per 1 compound formula (they are above the dashed horizontal lines). A similar utilization of more than 1 electron per mol was already observed in Li_2MnSiO_4 [17]. There we explained this important effect by the possibility of utilization of the Mn^{3+}/Mn^{4+} transition. A similar explanation could be adopted in the present context. However, looking at the shape of the charge–discharge curves for LNT100 and LMT20_CC (see Figs. 4 and 6), we see quite a com-

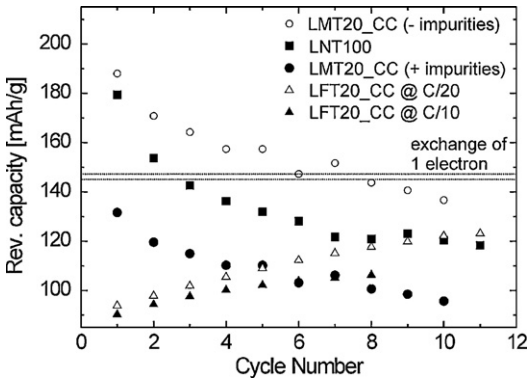

Fig. 7. Collection of the highest reversible capacities achieved so far for all three titanate materials. In all cases the temperature was 60 °C. The cycling rate was C/10, except for open triangles (C/20). In the Mn analogue, the impurities (30 wt.%) were either considered as part of active material (solid circles) or subtracted (open circles). The upper and lower dotted horizontal lines show the theoretical capacity for the Mn and Ni analogue, respectively (assuming the exchange of 1 electron per formula). The capacities are defined as discharge capacities whereby only the mass of active compound is considered.

plex behaviour with several changes in the slopes of curves. Thus, before any conclusive statements can be made, extensive research of general and local structural changes occurring during charge and discharge has to be carried out.

As regards the Fe analogue, the curve shape is much simpler and effectively exhibits only one redox reaction within the conditions used (see Figs. 4 and 6). It is reasonable to ascribe this reaction to the Fe^{2+}/Fe^{3+} pair. At C/10 its utilization is moderate, about 61% (90 mA hg^{-1}) in the first cycle. Interestingly, the capacity is gradually increasing during the further cycling to reach about 72% (106 mA hg^{-1}) after 8 cycles (Fig. 7, solid triangles). Such an increase in capacity with cycling is very reproducible, as seen in another cell measured at C/20 (there a capacity of 123 mA hg^{-1} was reached after 11 cycles which is 83% of the theoretical value). Such an initial capacity increase has previously been observed in $LiFePO_4$ olivines when embedded into a native carbon coating [14,18] but not in native carbon-free $LiFePO_4$ [18,19]. By analogy, we attribute the increasing capacity in Fig. 7 (triangles) to the quite large amount of native carbon black (15 wt.%) in the LFT20_CC sample. A possible mechanism explaining the effect of carbon on cycling behaviour has recently been proposed by Kerlau et al. [20]. Regardless of that, we may conclude that an important advantage of the Fe analogue could be its stability during cycling—both at low and high temperatures. Another obvious advantage of LFT20_CC is the smallest voltage hysteresis during charge–discharge. In the respect, the worst material is LNT100. It seems that this hysteresis is an inherent materials property and not a kinetic issue because decreasing the rate from C/10 (Fig. 4a) to C/2 (Fig. 6a) does not decrease significantly the hysteresis (the same can be found for the Mn analogue). Likewise, the effect of temperature on hysteresis is marginal (see Figs. 6a and c). So, essential changes in inherent materials properties (through doping, mixing, etc.) are probably needed to improve this drawback.

Finally, it is instructive to compare our results with those previously published by Prabaharan et al. [8]. We measured LNT100 at the same conditions, that is, using 20 wt.% of carbon black and measuring in the potential range of 2.5–4.8 V, at a rate of C/2 and at RT. The first-cycle results are very similar to those obtained by Prabaharan et al. [8] (Fig. 8a). The slightly lower reversible capacity in our material (90 mA hg^{-1} vs. 96 mA hg^{-1}) can be ascribed to the slightly bigger particles (average size about 100 nm as opposed to 75 nm in Prabaharan's et al. sample). The cycling behaviour was not reported by Prabaharan et al. [8]. We find it interesting that although in Fig. 8b the potential window is narrowed, the absolute values of capacity loss during cycling remains almost the same as observed in the wider potential window (see Fig. 4a, the graph for RT). In other words, narrowing the potential window at the lower margin from 1.95 to 2.5 V vs. Li only reduces the reversible capacity while the irreversible losses are not decreased.

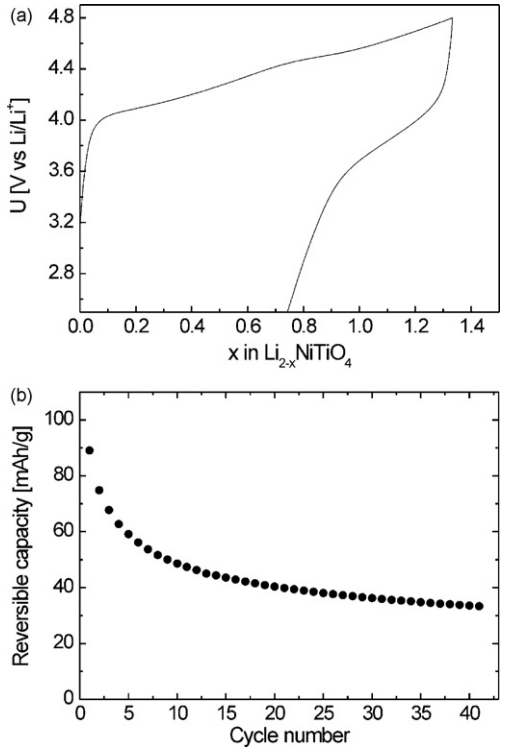

Fig. 8. Measurement of the present Li_2NiTiO_4 (LNT100) sample at the same conditions as published previously by Prabaharan et al. [8]; rate: C/2; temperature: 25 °C; voltage window: 2.5–4.8 V vs. lithium. (a) First charge–discharge cycle; (b) cycling performance in the first 40 cycles (not shown by Prabaharan et al. [8]).

4. Conclusions

In contrast to Li_2NiTiO_4 which works well at a particle size of ca. 100 nm, Li_2FeTiO_4 and Li_2MnTiO_4 only deliver a significant capacity if the particle size is much smaller—in our case from 10 to 25 nm. The reason is not a poor electronic conductivity—its value for Li_2FeTiO_4 (10^{-1} S cm^{-1} at RT) is even much higher than that for Li_2NiTiO_4 (10^{-8} S cm^{-1} at RT). This means that the main role of carbon coating in the present research is suppression of particle growth during heat treatment and, eventually, prevention of particle agglomeration. That the Fe and Mn analogues require much smaller particle size in order to become electrochemically active could be explained by assuming a lower ionic conductivity of these compounds if compared to the ionic conductivity of the Ni analogue.

At high temperatures, the Ni and Mn analogue can deliver very high reversible capacities in the first cycles (more than 1 electron per compound formula). However, both compounds tend to rapidly degrade at high temperatures. Both features resemble the behaviour of Li_2MnSiO_4, a compositionally related but structurally different compound. Conversely, the Fe analogue shows very good cycling stability but only allows an exchange of about 0.83 electrons per formula (at 7.4 mA g^{-1}). Based on the trends and explanations found in this paper, one could predict that a higher capacity would be delivered if the mean particle size of the titanate compounds is further decreased.

Acknowledgments

The financial support from the Slovenian Research Agency is fully acknowledged. Part of this work has been carried out in the framework of activities within the ALISTORE network of excellence. The authors also thank to Jože Moškon for performing the electric conductivity measurements.

References

[1] P.P. Prosini, M. Carewska, S. Scaccia, P. Wisniewski, M. Pasquali, Electrochim. Acta 48 (2003) 4205.
[2] A. Singhal, G. Skandan, G. Amatucci, F. Badway, N. Ye, A. Manthiram, H. Ye, J.J. Xu, J. Power Sources 129 (2004) 38.
[3] R. Dominko, M. Bele, M. Gaberscek, M. Remskar, D. Hanzel, J.M. Goupil, S. Pejovnik, J. Jamnik, J. Power Sources 153 (2006) 274.
[4] A. Nyten, A. Abouimrane, M. Armand, T. Gustafsson, J.O. Thomas, Electrochem. Commun. 7 (2005) 156.
[5] R. Dominko, M. Bele, M. Gaberscek, A. Meden, M. Remskar, J. Jamnik, Electrochem. Commun. 8 (2006) 217.
[6] M. Gaberscek, R. Dominko, M. Bele, M. Remskar, D. Hanzel, J. Jamnik, Solid State Ion. 176 (2005) 1801.
[7] J. Moskon, R. Dominko, M. Gaberscek, R. Cerc-Korosec, J. Jamnik, J. Electrochem. Soc. 153 (2006) A1805.
[8] S.R.S. Prabaharan, M.S. Michael, H. Ikuta, Y. Uchimoto, M. Wakihara, Solid State Ion. 172 (2004) 39.
[9] L.H. Brixner, J. Inorg. Nucl. Chem. 16 (1960) 162.

[10] M.V.V.M. Satya Kishore, S. Marinel, V. Pralong, V. Caignaert, S. D'Astorg, B. Raveau, Mater. Res. Bull. 41 (2006) 1378.
[11] L. Sebastian, J. Gopalakrishnan, J. Solid State Chem. 172 (2003) 171.
[12] M. Gaberscek, R. Dominko, J. Jamnik, Electrochem. Commun. 9 (2007) 2778.
[13] M. Kuezma, R. Dominko, M. Bele, M. Gaberscek, J. Jamnik, Patent Application P-200800065, Slovenia (2008).
[14] R. Dominko, M. Bele, M. Gaberscek, M. Remskar, D. Hanzel, S. Pejovnik, J. Jamnik, J. Electrochem. Soc. 152 (2005) A607.
[15] R. Amin, P. Balaya, J. Maier, Electrochem. Solid-State Lett. 10 (2007) A13.
[16] C. Delacourt, L. Laffont, R. Bouchet, C. Wurm, J.-B. Leriche, M. Morcrette, J.-M. Tarascon, C. Masquelier, J. Electrochem. Soc. 152 (2005) A913.
[17] A. Kokalj, R. Dominko, G. Mali, A. Meden, M. Gaberscek, J. Jamnik, Chem. Mater. 19 (2007) 3633.
[18] H.C. Shin, W.I. Cho, H. Jang, J. Power Sources 159 (2006) 1383.
[19] C. Delacourt, P. Poizot, S. Levasseur, C. Masquelier, Electrochem. Solid-State Lett. 9 (2006) A352.
[20] M. Kerlau, M. Marcinek, V. Srinivasan, R.M. Kostecki, Electrochim. Acta 52 (2007) 5422.